Inorganic Chemistry

Article

pubs.acs.org/IC

Manipulating the Excited States of Cyclometalated Iridium Complexes with β-Ketoiminate and β-Diketiminate Ligands

Yousf K. Radwan, Ayan Maity, and Thomas S. Teets*

Department of Chemistry, University of Houston, 112 Fleming Building, Houston, Texas 77204-5003, United States

Supporting Information

ABSTRACT: A series of cyclometalated iridium complexes with β-ketoiminate and β-diketiminate ligands are described. Two different cyclometalating (C^N) ligands—2-phenylpridine (ppy) and 2-phenylbenzothiazole (bt)—are used in concert with three different ancillary (LX) ligands—a phenyl-substituted β-ketoiminate ($acNac^{Me}$), a phenyl-substituted β-diketiminate ($NacNac^{Me}$), and a fluorinated version of the β-diketiminate ($NacNac^{CF_3}$)—to furnish a suite of six complexes. The complexes are prepared by metathesis reactions of chloro-bridged dimers $[Ir(C^N)_2(\mu\text{-}Cl)]_2$ with potassium or lithium salts of the ancillary LX ligand. Four of the complexes are characterized by X-ray crystallography, and all six were subjected to in-depth optical and electrochemical interrogation. Cyclic voltammetry shows both reduction and oxidation waves, with the latter strongly dependent on the identity of the LX ligand. The complexes are all luminescent, with the nature of the emissive excited state and the quantum yield (Φ) dependent on the identity of both the C^N and LX ligands. Whereas the complexes $Ir(ppy)_2(NacNac^{Me})$ and $Ir(ppy)_2(acNac^{Me})$ are weakly luminescent ($\Phi \approx 0.01$), the complexes $Ir(bt)_2(NacNac^{Me})$ and $Ir(bt)_2(acNac^{Me})$ are strongly luminescent, with the latter's quantum efficiency ($\Phi = 0.82$) among the highest ever observed for cyclometalated iridium complexes. Fluorination of the NacNac ligand gives rise to completely disparate emission behavior suggestive of a NacNac-centered emissive state. The results described here, in comparison with previous groups' studies on acetylacetonate (acac) analogues, suggest that the weaker-field NacNac and acNac ligands raise the energy of the metal-centered HOMO, with energy of the HOMO increasing in the order $NacNac^{CF_3}$ < $acNac^{Me}$ < $NacNac^{Me}$.

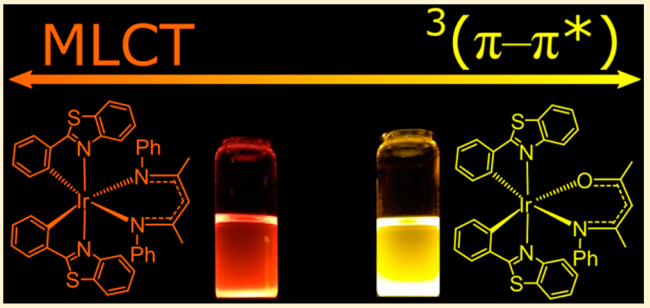

INTRODUCTION

Complexes of second- and third-row transition metals, typically featuring chelating diimine and/or cyclometalating ligands, are long heralded for their excited-state properties. Efficient population of triplet excited states, brought on by absorption of visible light and facilitated by spin−orbit coupling engendered by the heavy transition metal, gives rise to numerous applications for these complexes, including photoredox catalysis,[1−3] bioimaging,[4−7] and perhaps most prominently, organic light-emitting diodes (OLEDs).[8−10]

The excited states of these complexes are primarily comprised of mixed ligand-centered (LC) and metal-to-ligand charge transfer (MLCT) character, and as such alteration of the ligand environment can have a profound impact on the excited-state energies and dynamics. Cyclometalated complexes of iridium(III) in particular are a well-studied class of organometallic phosphors where synthetic control of excited-state properties has been demonstrated in numerous contexts. Figure 1 summarizes the major structural classes of cyclometalated iridium complexes. Whereas highly phosphorescent tris-cyclometalated complexes of the type *fac*-$Ir(C^N)_3$ are known for select cyclometalating ligands,[11,12] syntheses of such complexes are not always general or high-yielding, notwithstanding some notable recent developments.[13] As such, heteroleptic complexes

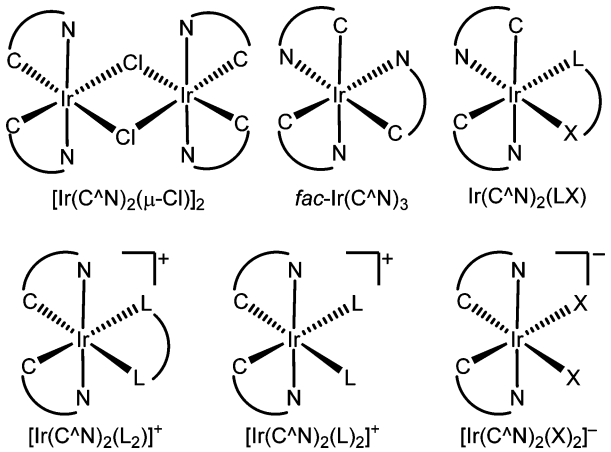

Figure 1. Major structural classes of cyclometalated iridium(III) complexes.

have been extensively targeted, where dimers of the type $[Ir(C^N)_2(\mu\text{-}Cl)]_2$ are cleaved by a combination of neutral "L" and anionic "X" ligands, or by bidentate L_2 or LX ligands,

Received: June 22, 2015
Published: July 9, 2015

DOI: 10.1021/acs.inorgchem.5b01401
Inorg. Chem. 2015, 54, 7122−7131

furnishing mononuclear, octahedral complexes (Figure 1). A particularly fruitful class of complexes, especially in the realm of OLEDs, has been $Ir(C^N)_2(acac)$, where acac is acetylacetonate or a substituted variant.[8,9,14] Synthetic control of electrochemical and optical properties in these complexes has been extensively demonstrated by alteration of the C^N ligand,[9,12,14] but it has also been shown that variation of ancillary ligands, be they monodentate or bidentate, can lead to substantially perturbed electronic structures.[8,10,15−18] From a simplistic standpoint, substitution of the C^N ligand has a profound impact on the energy of the unoccupied ligand-centered π^* levels, whereas exchange of the other ancillary ligand(s) in these heteroleptic complexes perturbs the energy of the metal-centered HOMO. In turn, this frontier orbital spacing influences the extent to which MLCT and LC states contribute to the emissive excited state.

Excepting a recent patent,[19] the use of β-ketoiminate (acNac) and β-diketiminate (NacNac) scaffolds as ancillary ligands for organometallic phosphors remains unexplored. Structurally analogous to the ubiquitous acac ligand, acNac and especially NacNac ligands have found widespread use as supporting ligands[20] in polymerization,[21−23] main-group,[24,25] and small-molecule activation chemistry.[26−31] Compared to acac, where substitution is only possible on the ligand "backbone", acNac and NacNac ligands afford greater control over their steric and electronic properties, owing to the presence of a substituent on the nitrogen atom(s) proximate to the metal center. For these reasons, acNac and NacNac ligands appear to be attractive ancillary ligands for cyclometalated iridium complexes, where the donicity of the ligand influences the energy and character of the emissive excited state, and its steric parameters may play a role in the excited-state dynamics.

In this work, we outline a class of cyclometalated iridium complexes supported by phenyl-substituted β-ketoiminate ($acNac^{Me}$) and β-diketiminate ($NacNac^{Me}$ and $NacNac^{CF_3}$) ligands (the superscript in the ligand notation denotes the backbone substituent). The syntheses of these new compounds are described, as well as structural characterization of four of them by single-crystal X-ray diffraction. The optical and electrochemical properties of the new complexes are demonstrably influenced by the ancillary ligand. Incorporation of these ligands into 2-phenylpyridine (ppy) derivatives largely quenches the room-temperature emission. However, complexes with 2-phenylbenzothiazole (bt) as the cyclometalating ligand show exceptionally efficient phosphorescence when supported by acNac or unfluorinated NacNac, highlighted by a quantum yield (Φ) of 0.82 for $Ir(bt)_2(acNac^{Me})$. By comparing analogous compounds with acac, acNac, and NacNac supporting ligands, we show, in our results, that the energy of the metal-centered HOMO systematically increases as additional nitrogen atoms are incorporated. Moreover, we show that fluorination of the backbone of the NacNac ligand reverses this trend, substantially lowering the HOMO energy relative to the unfluorinated versions, and also dramatically perturbs the energy and character of the low-energy excited state. This work demonstrates the potential value of acNac and NacNac ancillary ligands for cyclometalated iridium phosphors, providing another means of tailoring the electronic properties of this important class of complexes.

RESULTS

Synthesis of Complexes. Figure 2 shows the cyclometalating (C^N) and ancillary (LX) ligands employed here,

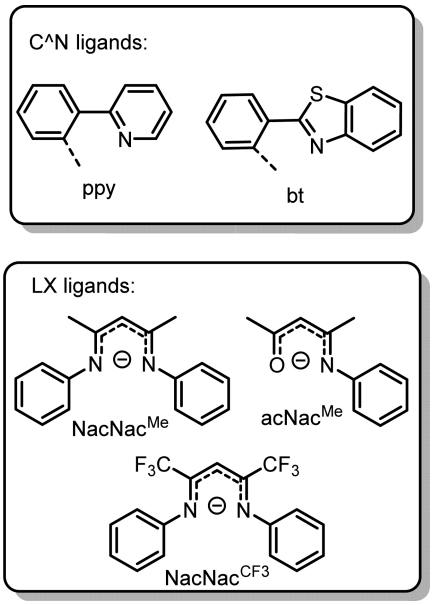

Figure 2. Abbreviations for C^N and LX ligands.

along with the abbreviations that will be used throughout. The syntheses of the complexes and their numerical designations are outlined in Scheme 1. The dimers $[Ir(C^N)_2(\mu\text{-}Cl)]_2$ are

Scheme 1. Synthesis of complexes 1−6

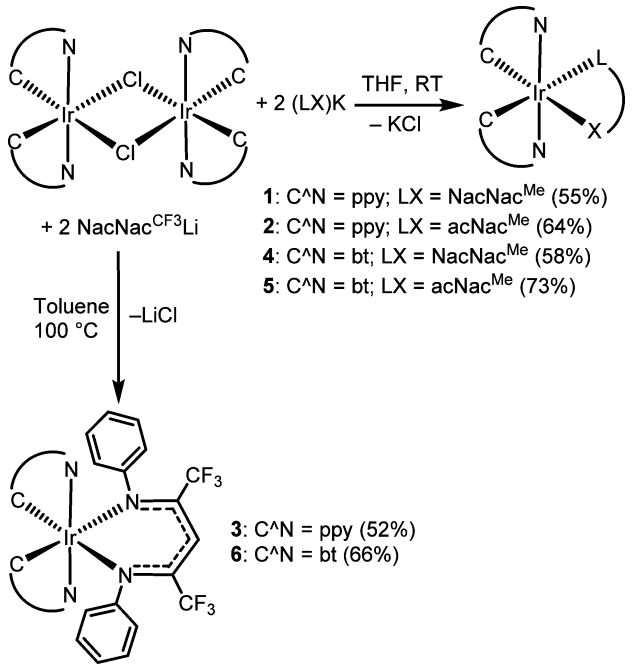

treated with $NacNac^{Me}K$ or $acNac^{Me}K$ at room temperature in THF to afford complexes **1**, **2**, **4**, and **5** in moderate yields. In a slight departure from these general conditions, complexes **3** and **6** are accessed by reacting the chloro-bridged dimers with $NacNac^{CF_3}Li$ in toluene at 100 °C.

The identity and purity of complexes **1**−**6** are readily determined by ^1H and $^{13}C\{^1H\}$ NMR spectroscopy. For NacNac-appended complexes **1**, **3**, **4**, and **6**, the C_2 symmetry of the complexes is readily ascertained. A single set of resonances attributed to the C^N ligand is observed in both

DOI: 10.1021/acs.inorgchem.5b01401
Inorg. Chem. 2015, 54, 7122−7131

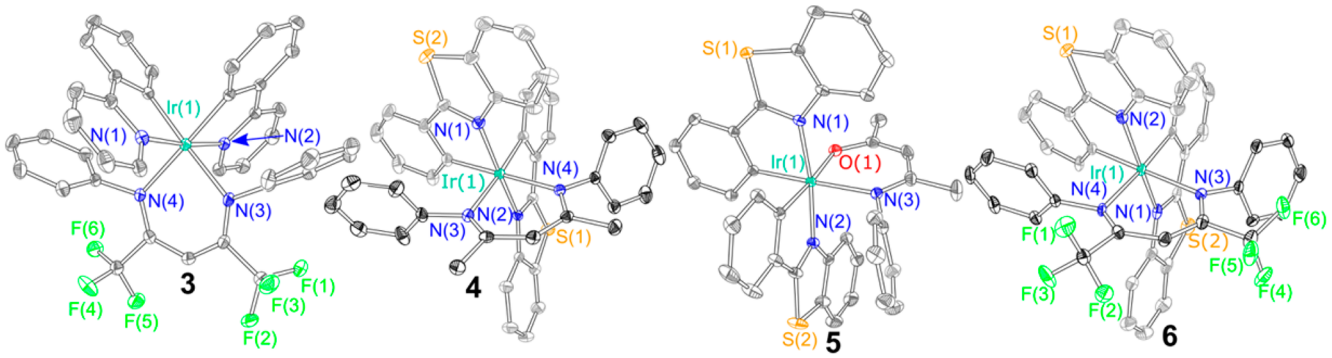

Figure 3. X-ray crystal structures of complexes **3**–**6**. Ellipsoids are drawn at the 50% probability level, with hydrogen atoms and solvate molecules omitted. For NacNac complexes **4** and **6**, the carbon atoms of the NacNac are shaded darker to aid interpretation.

the ^{1}H and $^{13}C\{^{1}H\}$ NMR spectra. For NacNac^{Me} complexes, one CH_3 resonance is present, and for NacNac^{CF_3} complexes the ^{19}F and $^{13}C\{^{1}H\}$ NMR spectra each show a single CF_3 resonance, with strong coupling to ^{19}F ($J \approx 290$ Hz) observed in the latter. In contrast, the asymmetry of acNac^{Me} complexes **2** and **5** is apparent in the NMR spectra. In addition to a much more complex aromatic region in the ^{1}H NMR, where each C^N proton is unique, the $^{13}C\{^{1}H\}$ NMR shows a unique resonance for each carbon in the molecule, 33 for ppy-substituted **2**, and 37 for bt variant **5**. For all six complexes, the $^{13}C\{^{1}H\}$ NMR spectra suggest that the *N*-phenyl substituents are static at room temperature, as six unique resonances are observed for these groups; only four such signals are seen in the spectra of the alkali metal ligand precursors.

Whereas complexes **1** and **2** were recalcitrant to characterization by single-crystal X-ray diffraction, complexes **3**–**6** all grew as single crystals by diffusion of pentane vapors into concentrated THF solutions. The structures are depicted in Figure 3, and Tables S1 and S2 in the Supporting Information summarize the crystallographic data. The crystal structures all show the expected octahedral geometry, and in the cases of the bt complexes the trans disposition of the C^N nitrogen atoms is unambiguous. In the bt complexes, the benzo substituents reside in grooves above and below the planes of the LX ligand backbone. The *N*-phenyl substituents on the LX ligand lie in close proximity to the C^N phenyl group, with centroid-to-centroid distances ranging between 3.4 and 3.8 Å. However, the two rings are always slightly canted, with the smallest dihedral angle being 16.4° in complex **6**, indicating that the two adjacent phenyl rings are not engaged in $\pi-\pi$ stacking. Comparing the structures of **4** and **6**, where backbone fluorination is introduced in the latter, we see average Ir–N(NacNac) internuclear distances of 2.168(2) Å in **4** and 2.192(4) Å in **6**, revealing a small but significant effect of fluorination on the bond distances to the iridium. The average Ir–C bond distance is 2.026(2) Å in NacNac^{Me} complex **4**, and 2.018(5) Å in NacNac^{CF_3} complex **6**, indicating no significant difference in the trans influence of the fluorinated and unfluorinated NacNac ligands. For complex **5**, the Ir–C bond distance trans to the oxygen is 2.0085(19) Å, and a value of 2.0084(18) Å is observed trans to nitrogen, showing that the asymmetry of the acNac ligand does not induce disparate Ir–C bond distances.

Electrochemistry. Figure 4 shows overlaid cyclic voltammograms of the complexes, arranged by C^N ligand. The electrochemical oxidation potentials are also summarized in Table 1, along with those for related acac complexes. All six complexes introduced in this work display reversible oxidation

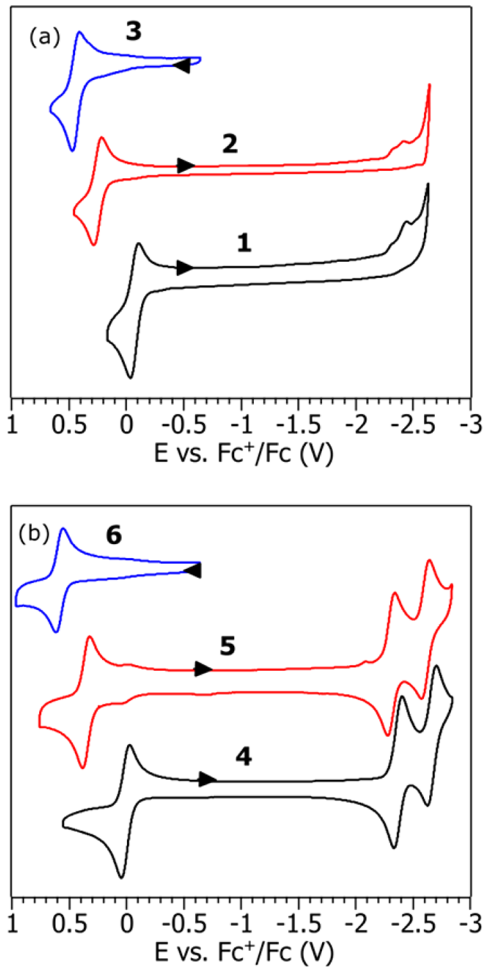

Figure 4. Overlaid cyclic voltammograms of (a) ppy complexes **1**–**3** and (b) bt complexes **4**–**6**. The CVs were recorded in MeCN with 0.1 M NBu_4PF_6 electrolyte using a glassy carbon working electrode and a scan rate of 0.1 V/s. Currents are normalized to put the individual traces on the same scale, and the arrows show the approximate starting potentials and scan direction.

waves to formally Ir^{IV} oxidation states, with half-wave potentials that are strongly dependent on the identity of the LX ligand. Complexes supported by NacNac^{Me} are comparatively easy to oxidize, with potentials very near that of the ferrocenium/ferrocene couple. Referenced to Fc^+/Fc, the oxidation potential for Ir(ppy)$_2$(NacNac^{Me}) (**1**) is −0.07 V, and that of Ir(bt)$_2$(NacNac^{Me}) (**4**) is 80 mV more positive, at +0.01 V.

DOI: 10.1021/acs.inorgchem.5b01401
Inorg. Chem. 2015, 54, 7122–7131

Table 1. Summary of Electrochemical and Optical Data for All Complexes

complex	$E_{1/2}(Ir^{IV}/Ir^{III})$, V vs Fc/Fc^+	absorbance,[a] λ, nm ($\varepsilon/10^3$)	emission, λ, nm		quantum yield[a] (Φ)	$E_{1/2}(Ir^{IV}/{}^*Ir^{III})$, V vs Fc/Fc^+
			at 293 K[a]	at 77 K[b]		
$Ir(ppy)_2(acac)$[c]	+0.46	260 (32), 345 (6.3), 412 (2.5), 460 (2.0), 497 (1.0)	516	not reported	0.34	−1.9[d]
1	−0.07	264 (39), 357 (12), 383 (11), 460 (sh) (1.8)	569	522, 554 (sh)	0.013	−2.4
2	+0.25	262 (42), 309 (sh) (17), 344 (11), 378 (sh) (7.4), 455 (sh) (2.4), 492 (1.4)	564	505, 540	0.0084	−2.2
3	+0.44	267 (37), 334 (sh) (13), 399 (9), 417 (sh) (8.4), 479 (sh) (3.9)	[e]	496, 523, 563, 667, 738, 813	[e]	−2.1, −1.4[f]
$Ir(bt)_2(acac)$[c]	0.59	269 (40), 313 (25), 327 (32), 408 (6.3), 447 (6.3), 493 (2.5), 540 (1.0)	557	not reported	0.26	−1.6[d]
4	+0.01	269 (34), 291 (sh) (28), 311 (31), 322 (32), 383 (17), 452 (4.6)	636	590, 638, 691 (sh)	0.21	−2.1
5	+0.35	277 (35), 310 (30), 323 (32), 339 (sh) (21), 365 (sh) (11), 410 (sh) (5.9), 493 (sh) (3.7)	571, 610 (sh)	554, 602, 655, 715 (sh)	0.82	−1.9
6	+0.59	262 (36), 269 (35), 313 (sh) (32), 322 (37), 418 (13), 452 (sh) (8.5)	[e]	521 (sh), 554, 593, 682, 755, 823 (sh)	[e]	−1.8, −1.2[f]

[a]Recorded in 2-MeTHF (acac complexes) or THF (**1**–**6**) at 293 K. [b]Solvent is toluene. [c]Data from ref 14. Redox potentials originally reported vs Ag/AgCl. [d]From data tabulated in refs 14 and 32. [e]Nonemissive at room temperature. [f]Values for the two distinct emissive states.

Substitution of $acNac^{Me}$ induces a ca. 300 mV positive shift in the oxidation potential, with $E_{1/2}$ values of +0.25 and +0.35 V observed for **2** and **5**, respectively. Fluorination of the NacNac ligand results in an additional ca. 200 mV potential shift, with oxidation potentials of +0.44 and +0.59 V in complexes **3** and **6**. In all cases we observe that bt-ligated complexes show more positive oxidation potentials relative to the ppy analogues, and that the oxidation waves in the bt series are somewhat more sensitive to substitution of the LX ligand.

Excited-state redox potentials were estimated for the compounds described here and are included in Table 1. The excited-state energies (E_{0-0}) were estimated from 77 K emission spectra (vide infra) and combined with the formal Ir^{IV}/Ir^{III} potentials to furnish estimates of the excited-state reduction potentials, $E_{1/2}(Ir^{IV}/{}^*Ir^{III})$.[33] The trends mirror those of the ground-state potentials, with the NacNac- and acNac-appended complexes showing more negative excited-state $E_{1/2}$ values than the corresponding acac derivatives.

The complexes are reduced at negative potential values. Complexes with $NacNac^{CF_3}$ show complex, irreversible reduction waves with large current values. These reductive features indicate instability of the fluorinated ligand at negative potentials, and are not shown in Figure 4 or considered further. Unfluorinated complexes show much more well-behaved reduction features, with very similar onset potentials for all four examples. In the case of ppy complexes **1** and **2**, two closely spaced irreversible features are observed, with onset potentials of ca. −2.2 V. For bt complexes **4** and **5**, two reversible reduction waves are noted, with potentials that depend slightly on the identity of the LX ligand. For $Ir(bt)_2(NacNac^{Me})$ (**4**), the $E_{1/2}$ values for these reduction waves are −2.37 and −2.66 V vs Fc^+/Fc, and for $Ir(bt)_2(acNac^{Me})$ (**5**) the values are −2.31 and −2.61 V.

Optical Properties. Table 1 summarizes the UV–vis absorption and emission spectra of complexes **1**–**6**. The room-temperature absorption and emission spectra of unfluorinated complexes **1**, **2**, **4**, and **5** are overlaid in Figure 5. In addition, spectra for individual complexes are collected in the Supporting Information. The absorption spectra show several overlapping bands, with some absorption tailing into the visible region and giving rise to the yellow-orange (C^N = ppy) to red-orange (C^N = bt) colors of the complexes. Strong bands in the UV region, whose positions and intensities are almost exclusively dependent on the identity of the cyclometalating ligand, appear for all complexes. All have a strong band between 260 and 277 nm, and the bt complexes possess additional sharp, intense absorptions near 310–320 nm. These high-

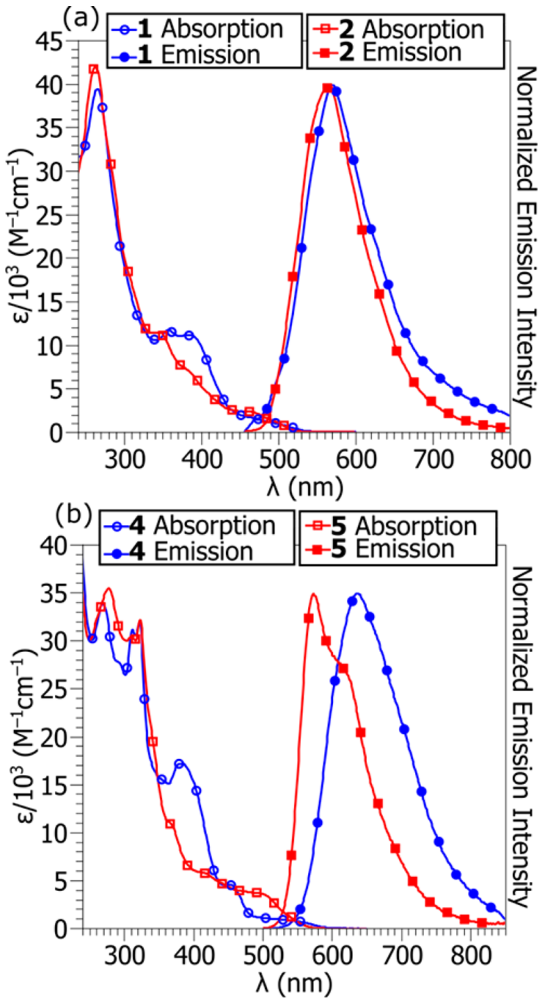

Figure 5. Overlaid UV–vis absorption and emission spectra of (a) ppy complexes **1** and **2** and (b) bt complexes **4** and **5**. The spectra were recorded at room temperature in deoxygenated THF solutions. For emission spectra, samples were excited at λ = 420 nm.

DOI: 10.1021/acs.inorgchem.5b01401
Inorg. Chem. 2015, 54, 7122–7131

energy features are assigned to $^1(\pi-\pi^*)$ transitions in the C^N ligand. In the near-UV and visible regions, the appearance of the spectra depends on the identity of the LX ligand. Complexes **1** and **4**, which have NacNac^{Me} as the LX ligand, show intense bands at 383 nm, with ε = 11 000 (**1**) and 17 000 M^{-1} cm^{-1} (**4**). These bands are considerably diminished in acNac^{Me} complexes **2** and **5**, although shoulders are still apparent at these wavelengths.

The room-temperature emission spectra of complexes **1**, **2**, **4**, and **5**, measured in THF, are also shown in Figure 5. Excitation spectra are collected in the Supporting Information, and match well with the absorption features. The room-temperature spectra of Ir(ppy)$_2$(NacNac^{Me}) (**1**) and Ir(ppy)$_2$(acNac^{Me}) (**2**) are nearly identical. Both have broad, featureless bands, with λ_{max} = 569 nm for **1** and 564 nm for **2**, and both are only weakly luminescent, with Φ = 0.013 (**1**) and 0.0084 (**2**). In contrast, bt complexes **4** and **5** are intensely luminescent at room temperature, and the energy and shape of the emission band depends strongly on the identity of the LX ligand. For Ir(bt)$_2$(NacNac^{Me}) (**4**), a single broad band with λ_{max} = 636 nm is observed, with Φ = 0.21. In the case of Ir(bt)$_2$(acNac^{Me}) (**5**), vibronic structure is evident even at room temperature, with λ_{max} = 571 nm and a shoulder at 610 nm, and Φ = 0.82.

Additional insight into the emissive excited state is gained by studying rigidochromic shifts of the emission spectra. The spectra of complexes **1**, **2**, **4**, and **5** were also recorded in toluene, at 293 K in fluid solution and at 77 K in a rigid solvent glass. The results are shown in Figure 6, and summarized in Table 1. The room-temperature spectra in toluene (Figure 6) are nearly identical to those in THF (Figure 5). Upon cooling to 77 K, marked changes are noted in the emission spectra. For ppy complexes **1** and **2**, a significant hypsochromic shift in λ_{max} is seen upon cooling, with vibronic structure evident at 77 K. The emission maximum shifts from 565 to 522 nm when cooling a solution of Ir(ppy)$_2$(NacNac^{Me}) (**1**) from 293 to 77 K, and a shift from 563 to 505 nm is seen when Ir(ppy)$_2$(acNac^{Me}) (**2**) is subjected to the same treatment. The rigidochromic behavior of bt complexes **4** and **5** are similar, though the shifts are less dramatic. For NacNac^{Me} complex **4**, a hypsochromic shift in λ_{max} is observed with cooling, from 615 to 590 nm, and some vibronic structure is evident at low temperature. In the case of Ir(bt)$_2$(acNac^{Me}) (**5**), cooling to 77 K results in a small (14 nm) hypsochromic shift in λ_{max}, and the vibronic structure becomes more well-resolved.

The optical properties of NacNac^{CF_3} complexes **3** and **6** are markedly different than the unfluorinated complexes, particularly in the emission spectra. Figure 7 shows the overlaid spectra of complexes **3** and **6**. The absorption spectra are qualitatively similar to those of the other complexes, with analogous $^1(\pi-\pi^*)$ transitions evident in the UV, and what are likely MLCT transitions at lower energy. The visible absorption in these complexes is more intense than that of the unfluorinated species, although the peak positions are very similar. The emission spectra of **3** and **6** are quite distinct, however. At room temperature the complexes are nonemissive, in either THF or toluene solution. However, in toluene at 77 K intense emission occurs that covers most of the visible region. Both complexes seem to have two distinct emission bands; at higher energy a less intense band with some vibronic fine structure is observed. The position of this band depends on the identity of the C^N ligand. In ppy complex **3**, this first band has maxima at 496, 523, and 563 nm, and substitution of bt in complex **6** gives a band with maxima at 521, 554, and 593 nm.

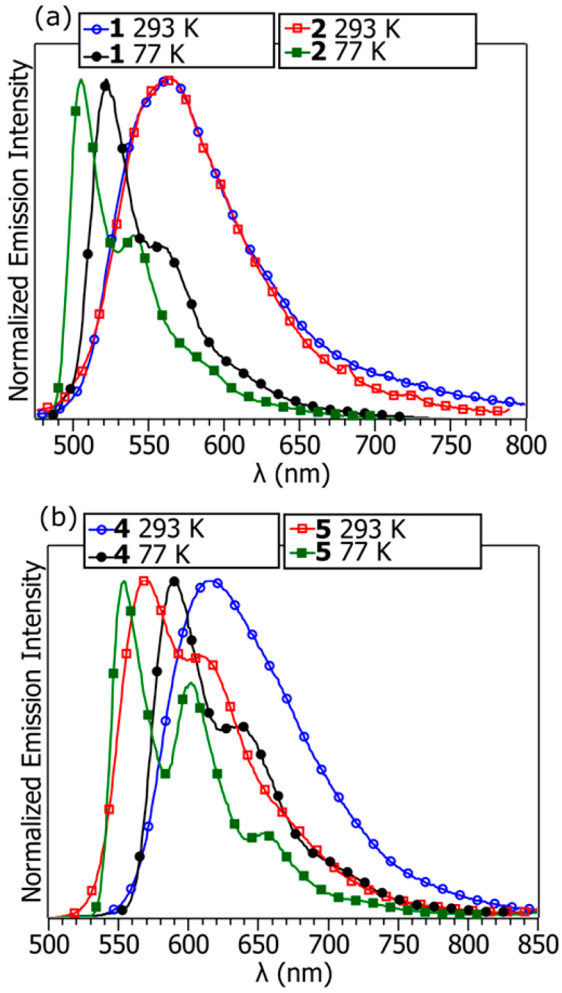

Figure 6. Emission spectra of (a) **1** and **2** and (b) **4** and **5**, recorded in toluene at 293 and 77 K. Samples were excited at 420 nm, excepting complex **2** which was excited at 400 nm in the room-temperature spectrum.

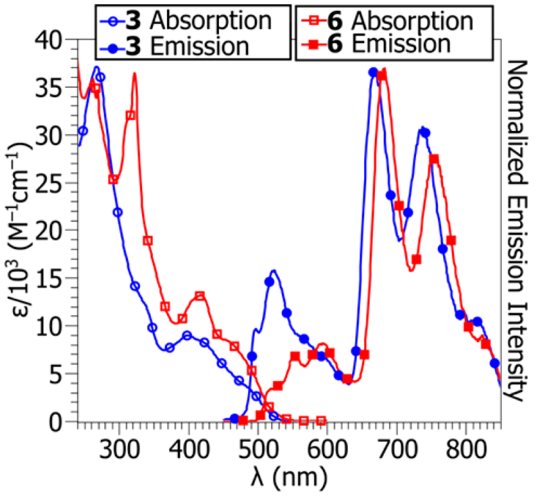

Figure 7. UV−vis absorption and emission spectra of NacNac^{CF_3} complexes **3** and **6**. The absorption spectra were recorded in THF at room temperature, and the emission spectra in toluene at 77 K. For emission spectra, λ_{ex} = 400 nm (**3**) and 430 nm (**6**).

In the red to near-infrared region of the spectrum, both **3** and **6** possess even more intense emission bands, also with vibronic

DOI: 10.1021/acs.inorgchem.5b01401
Inorg. Chem. 2015, 54, 7122−7131

structure. These bands are less sensitive to the identity of the C^N ligand, appearing at 667, 738, and 813 nm in ppy complex **3** and shift to 682, 755, and 823 nm in bt complex **6**. The two emission bands in **3** and **6** have distinct excitation profiles, as shown in Figures S8, S9, S17, and S18 in the Supporting Information. In both cases, the low-energy emission bands are more strongly stimulated by visible excitation, as compared to the higher-energy emission bands.

DISCUSSION

Structurally related to acetylacetonate (acac), which has long been used as an ancillary "LX" ligand in monomeric cyclometalated iridium phosphors,[9,14] β-ketoiminate (acNac) and β-diketiminate (NacNac) ligands have been little explored in this context.[19] In fact, compounds of iridium with acNac[34,35] or NacNac[36,37] ligands are rare in general, with most of the best-known recent examples being carbonyl or olefin/hydride complexes. Whereas the complexes $Ir(C^N)_2(acac)$ are generally prepared by treatment of $[Ir(C^N)_2(\mu\text{-}Cl)]_2$ with the appropriate acetylacetone (acacH) at elevated temperatures in the presence of a weak base like sodium carbonate, our initial attempts at duplicating these conditions with $NacNac^{Me}H$ resulted in sluggish reactions and poor yields of the desired product. We instead found that, in the case of unfluorinated acNac and NacNac ligands, the desired complexes could be prepared in moderate to good isolated yields at room temperature, utilizing a stoichiometric amount of the potassium salt of the LX ligand in THF (Scheme 1). This route proved to be general, and allowed preparation of complexes **1**, **2**, **4**, and **5** in yields of 55−73% with reaction times of ∼2 h. In contrast, we were unable to access $NacNac^{CF_3}K$ in pure form, prompting us to switch to the lithium salt for the installation of this ancillary ligand. This less reactive precursor required elevated temperatures (100 °C) for metathesis to occur, but nonetheless we were able to isolate two $Ir(C^N)_2(NacNac^{CF_3})$ complexes in moderate yields (52 and 66%) and high purities.

Four of the complexes, **3**−**6**, were characterized by single-crystal X-ray diffraction, confirming the structures that were assigned by ^1H and $^{13}C\{^1H\}$ NMR spectroscopies. In general, the identity of the LX ligand has little effect on the observed bond lengths and angles at the iridium center. One exception is found in comparing the structures of **4** and **6**, where fluorination of the NacNac ligand in the latter results in slightly longer (0.024 Å on average) bond distances between the iridium and the NacNac nitrogens. This may be reflective of diminished π donation in the latter, although the effect is modest.

Despite the miniscule structural perturbations brought on by substitution of LX ligands, the influence of the acNac and NacNac supporting ligands on the electronic structures of the complexes is profound. As is typical for cyclometalated iridium complexes,[9,14,15] all of the reported complexes show a reversible oxidation wave, the potential of which depends on the identity of the LX ligand. The unfluorinated complexes described here (**1**, **2**, **4**, and **5**) are more easily oxidized than previously reported cyclometalated iridium complexes supported by acac[14] or other LX ligands.[15,38] Substitution of $NacNac^{Me}$ for $acNac^{Me}$ and $NacNac^{CF_3}$ progressively shifts the oxidation to more positive potentials, with the potentials for fluorinated complexes **3** and **6** more positive by 510 and 580 mV relative to their unfluorinated congeners **1** and **4**. All of these results are consistent with the nature of the LX ligand strongly influencing the energy of the metal-centered HOMO. Successive addition of nitrogen donors on moving from acac to acNac to NacNac increases the π-donating ability of the LX ligand, and results in progressively higher HOMO energies and lower oxidation potentials. Fluorination of the NacNac must decrease the π donation substantially, as the oxidation potentials of the fluorinated complexes are comparable to those found with acac as the supporting ligand.

In addition to the ground-state potentials discussed above, excited-state reduction potentials can be estimated by combining the excited-state E_{0-0} energy with the ground-state potential.[33] The NacNac and acNac compounds described here are predicted to be stronger photoreductants than the corresponding acac derivatives.[14,32] Additionally, complex **1** is predicted to be ca. 200 mV more potent a photoreductant than *fac*-$Ir(ppy)_3$,[11,39] which has been extensively utilized in photoredox catalysis.[3,40,41] Both the excited-state energy and the ground-state $E_{1/2}(Ir^{IV}/Ir^{III})$ potential decrease when NacNac is added to the $Ir(C^N)_2^+$ fragment, but the larger decrease in the latter leads to more negative excited-state redox potentials.

Given the observed dependence of the HOMO energy on the LX ligand, it stands to reason that the nature of the excited state is altered upon incorporation of acNac and NacNac ancillary ligands. It is well established that the emissive excited state in cyclometalated iridium complexes is an admixture of ligand-centered (LC) $^3(\pi-\pi^*)$ and metal-to-ligand charge transfer (^{1}MLCT and ^{3}MLCT) states. The emission spectra observed here are all consistent with increased MLCT character upon substitution of nitrogen-containing acNac or NacNac ligands for acac. The emission energy, band shape, quantum yield, and rigidochromic behavior can provide insight into the qualitative contribution of the MLCT state to the emission.

The complex $Ir(ppy)_2(acac)$ has a room-temperature emission wavelength of 516 nm with a shoulder at slightly longer wavelength suggestive of vibronic structure, consistent with significant LC character (Φ = 0.34).[14] In contrast, the complexes $Ir(ppy)_2(NacNac^{Me})$ (**1**) and $Ir(ppy)_2(acNac^{Me})$ (**2**) show emission bands that are substantially red-shifted and broad, with no vibronic fine structure and much lower quantum yields ($\Phi \approx 0.01$). The spectra of **1** and **2** are nearly identical at room temperature, but they diverge somewhat at 77 K (Figure 6a) and show some vibronic structure at the lower temperature. Large rigidochromic effects are observed, with λ_{max} blue-shifting by 43 nm (**1**) and 58 nm (**2**). These shifts are considerably larger than the 12 nm hypsochromic shift observed in the related complex $Ir(tpy)_2(acac)$ (tpy = 2-*p*-tolylpyridine).[15] All of these observations are consistent with substantial MLCT character in the excited state, brought on by substitution of acNac and NacNac for acac.

NacNac and acNac ligands perturb the excited states of bt-ligated complexes to a lesser extent. With bt as the C^N ligand, the $^3(\pi-\pi^*)$ state lies lower in energy, and is expected to contribute more strongly to the low-energy excited state. The room-temperature emission spectrum of $Ir(bt)_2(acac)$ has λ_{max} = 557 nm and discernible vibronic fine structure. Substitution of $NacNac^{Me}$, in complex **4**, causes a sizable red shift and broadening of the emission spectrum, with λ_{max} = 636 nm and no fine structure resolved. These observations are consistent with enhanced MLCT character in complex **4**, although the 77 K emission spectrum, which shows a significant rigidochromic shift (λ_{max} = 615 nm at 293 K, 590 nm at 77 K) and some vibronic fine structure, is consistent with substantial contribution of both LC and MLCT states to the low-energy emitting

DOI: 10.1021/acs.inorgchem.5b01401
Inorg. Chem. 2015, 54, 7122−7131

excited state. The emission behavior of complex **5**, where LX = acNac^{Me}, is very similar to that of Ir(bt)$_2$(acac), with an only 14 nm bathochromic shift in the room-temperature emission maximum. At 77 K a slight hypsochromic shift and even sharper vibronic structure are observed, consistent with predominately LC excited-state character.

In contrast to Ir(ppy)$_2$(LX), where substitution of acNac and NacNac results in dramatically lower phosphorescence quantum yields, in the bt series of complexes incorporation of nitrogen-containing ligands preserves high phosphorescence efficiency. Ir(bt)$_2$(NacNac^{Me}) (**4**) has $\Phi = 0.21$, nearly identical to that of Ir(bt)$_2$(acac) ($\Phi = 0.26$), and in Ir(bt)$_2$(acNac^{Me}) (**5**) an impressive $\Phi = 0.82$ is observed, among the highest ever for cyclometalated iridium complexes, with only a few known complexes displaying comparable values. Monoanionic cyclometalated iridium complexes of the type $[Ir(ppy)_2(X)_2]^-$, where X = CN^-, NCS^-, and NCO^-, show emission maxima that depend slightly on the identity of the X^- ligand, in all cases with quantum yields greater than 0.75.[17] In addition, a class of cationic $[Ir(C\text{^}N)_2(LL)]^+$ complexes, where LL is a substituted bipyridine, also display high quantum yields with certain substitution patterns on the bipyridine.[42,43] In this latter work it was also shown that the quantum yield is enhanced when LC $\pi-\pi^*$ character is more extensively mixed with MLCT character in the low-energy emissive state. Consistent with this notion, we find that substitution of ppy for bt, which enhances the $\pi-\pi^*$ contribution, results in a dramatic increase in the emission quantum yield. Furthermore, when comparing NacNac complex **4** with acNac complex **5**, we see augmented LC character and a higher quantum yield in the latter. These observations reveal the possibility that nitrogen-containing acNac and NacNac ligands can be used to tune excited-state energies and characters, without sacrificing the efficient luminescence that cyclometalated iridium complexes are renowned for. Continued experimental and computational studies on these and related complexes will provide better insight into the factors that control the emission energies and quantum yields.

Fluorination of the NacNac ligand in complexes **3** and **6**, Ir(C^N)$_2$(NacNac^{CF_3}), gives rise to distinct emission spectra, suggesting a change in the nature of the low-energy excited states for these complexes. Nonemissive at room temperature, at 77 K two distinct emission bands with discernible fine structure are observed for both of these complexes. The two bands cover much of the visible spectrum, giving rise to emission that is very nearly white in color. Dual emission has been observed in a number of transition-metal complexes,[44−47] and the spectra of **3** and **6** suggest such behavior in these complexes. The higher energy band is consistent with an LC transition, bathochromically shifted by ∼1000 cm^{-1} when bt is substituted for ppy. The lower energy bands, which are completely absent in the unfluorinated complexes, are nearly identical in complexes **3** and **6**, have similar vibronic spacing to the high-energy band, and are only perturbed ∼300 cm^{-1} upon ppy in **3** is replaced with bt in **6**. The two bands give rise to distinct excitation profiles (see Supporting Information); the excitation spectra bear qualitative resemblance to the absorption spectra, but their disparate appearances suggest that the two emissive excited states are independently populated, via excitation of different absorption bands.[48] An analogous phenomenon has recently observed in a conjugated ruthenium−polypyridyl dimer.[44] Whereas the precise nature of the emissive states in **3** and **6** is not readily apparent from these preliminary studies, these observations are consistent with significant contribution of the NacNac^{CF_3} ligand to the low-energy excited state. Although applications may be limited because the emission is only active at low temperatures, we aim to further explore the potential of these complexes as broad-band emitters, all the while using further experimental and theoretical work on these and related complexes to unveil the character of the excited state that gives rise to this unexpected emission behavior.

The work described here shows the potential power of β-ketoiminate and β-diketiminate ligands to tune the emission of cyclometalated iridium complexes within the well-known excited-state manifold of these complexes, and also to introduce new emissive excited states. Both of these avenues hold promising implications and will be the subject of future work in this area.

EXPERIMENTAL SECTION

Materials. All reactions were executed in a nitrogen-filled glovebox operating at <1 ppm of O_2 and <1 ppm of H_2O, or in vessels sealed with Teflon plugs. Solvents for reactions and optical measurements were dried by the method of Grubbs,[49] passing through dual alumina columns on a commercial solvent purification system (SPS), and stored over 3A molecular sieves. All NMR solvents were dried and stored over 3A molecular sieves; $CDCl_3$ was also stored over potassium carbonate in addition to sieves. The compounds NacNac^{Me}H,[50] NacNac^{CF_3}H,[50,51] and benzylpotassium[52] were prepared according to literature procedures, whereas acNac^{Me}H was isolated as a side product in the synthesis of NacNac^{Me}H or prepared as described previously.[53] Potassium and lithium salts of the NacNac and acNac ligands were prepared following an analogous procedure to that used for bulky NacNac ligands;[54] details are provided below. Cyclometalated iridium dimers $[Ir(ppy)_2(\mu\text{-}Cl)]_2$ (ppy = 2-phenylpyridine) and $[Ir(bt)_2(\mu\text{-}Cl)]_2$ (bt = 2-phenylbenzothiazole) were prepared by refluxing $IrCl_3{\cdot}nH_2O$ with 2−2.5 equiv of the cyclometalating ligand in a 3:1 mixture of 2-methoxyethanol and water.[55] Tetrabutylammonium hexafluorophosphate ($TBAPF_6$) was recrystallized from hot ethanol and ferrocene was sublimed before use in electrochemical experiments.

Physical Methods. NMR spectra were recorded at room temperature using a JEOL ECA-600 NMR spectrometer. UV−vis absorption spectra were recorded in THF solutions in screw-capped quartz cuvettes using an Agilent Carey 60 UV−vis spectrophotometer. Emission spectra were recorded using a Horiba FluoroMax-4 spectrofluorometer, using appropriate long-pass filters to exclude stray excitation light from detection. Samples for room-temperature emission were housed in 1 cm quartz cuvettes with septum-sealed screw caps, and samples for low-temperature emission were contained in a custom quartz EPR tube with high-vacuum valve and immersed in liquid nitrogen using a finger dewar. Emission quantum yields[56] were determined relative to a standard of tetraphenylporphyrin in toluene, which has a reported fluorescence quantum yield (Φ_F) of 0.11.[57] Cyclic voltammetry (CV) measurements were performed with a CH Instruments 602E potentiostat interfaced with a nitrogen glovebox via wire feedthroughs. Samples were dissolved in acetonitrile with 0.1 M $TBAPF_6$ as a supporting electrolyte. A 3 mm diameter glassy carbon working electrode, a platinum wire counter electrode, and a silver wire pseudo-reference electrode were used. Potentials were referenced to an internal standard of ferrocene. Elemental analyses were performed by Atlantic Microlab, Inc.

Preparation of NacNac^{Me}K. In the glovebox, NacNac^{Me}H (500 mg, 2.00 mmol) was dissolved in 20 mL of Et_2O, giving a pale yellow solution. The solution was cooled with liquid nitrogen in the glovebox cold well for 30 min. After removing from the cold well, solid benzylpotassium (260 mg, 2.00 mmol, 1.00 equiv) was immediately added in a few portions. The red color of the benzylpotassium rapidly faded, and a bright yellow suspension resulted. The mixture was stirred for 1 h at room temperature, at which time the volatiles were removed

DOI: 10.1021/acs.inorgchem.5b01401
Inorg. Chem. 2015, 54, 7122−7131

in vacuo. The resulting canary yellow solid was suspended in hexane (~10 mL) and collected by vacuum filtration, washing with an additional 10 mL of hexane before drying in vacuo. Yield: 452 mg (78.5%). ^{1}H NMR (600 MHz, THF-d_8) δ: 7.03 (t, J = 7.5 Hz, 4H, ArH), 6.58−6.66 (m, 6H, ArH), 4.19 (s, 1H, PhNC(CH_3)CHC(CH_3)NPh), 1.71 (s, 6H, CH_3). ^{13}C{^{1}H} NMR (151 MHz, THF-d_8) δ: 159.7, 157.7, 128.7, 123.1, 118.9, 93.9, 22.9.

Preparation of acNac^{Me}K. In the glovebox, acNac^{Me}H (350 mg, 2.00 mmol) was dissolved in 20 mL of Et_2O. The colorless solution was frozen in the cold well. The frozen solution was removed, and upon melting benzylpotassium (260 mg, 2.00 mmol, 1.00 equiv) was added as a solid. A colorless suspension resulted, which was stirred at room temperature for 1 h. The volatiles were removed in vacuo, and the colorless solid was suspended in 10 mL of pentane and cooled to −35 °C. The cold mixture was filtered, and the product was washed with 4 mL of pentane and dried in vacuo. Yield: 261 mg (61.3%). ^{1}H NMR (400 MHz, THF-d_8) δ: 7.08 (t, J = 7.6 Hz, 2H, ArH), 6.75 (t, J = 7.2 Hz, 1H, ArH), 6.61 (d, J = 8.0 Hz, 2H, ArH), 4.50 (s, 1H, PhNC(CH_3)CHC(O)CH_3), 1.60 (br, s, 3H, CH_3), 1.56 (s, 3H, CH_3). ^{13}C{^{1}H} NMR (151 MHz, THF-d_8) δ: 181.0, 164.8, 155.8, 128.9, 122.6, 120.6, 95.0, 29.1, 22.0.

Preparation of NacNac^{CF_3}Li. A sample of NacNac^{CF_3}H (546 mg, 1.52 mmol) was dissolved in 10 mL of hexane and chilled in the glovebox freezer for 40 min (−35 °C). The solution was removed, and while cold a solution of n-BuLi (1.0 mL, 1.6 M, 1.6 mmol, 1.1 equiv) was added dropwise via syringe. A yellow solid formed immediately, and the mixture was stirred for 3 h at room temperature before placing in the freezer overnight. The solid was collected by filtration, washed with chilled pentane, and dried in vacuo. Yield: 487 mg (87.7%). ^{1}H NMR (600 MHz, C_6D_6) δ: 7.11 (t, J = 7.8 Hz, 4H, ArH), 6.94 (t, J = 7.2 Hz, 2H, ArH), 6.65 (d, J = 7.8 Hz, 4H, ArH), 6.01 (s, 1H, PhNC(CF_3)CHC(CF_3)NPh). ^{13}C{^{1}H} NMR (151 MHz, C_6D_6) δ: 152.4 (q, $^2J_{CF}$ = 24 Hz), 150.8, 128.6, 123.8, 123.5, 121.3 (q, $^2J_{CF}$ = 289 Hz), 83.3. ^{19}F NMR (565 MHz, C_6D_6) δ: −60.3.

Preparation of Ir(ppy)$_2$(NacNac^{Me}) (1). In the glovebox, [Ir(ppy)$_2$(μ-Cl)]$_2$ (100 mg, 0.0933 mmol) was suspended in 2 mL of THF. A solution of NacNac^{Me}K (54 mg, 0.19 mmol, 2.0 equiv) in 6 mL of THF was added via pipet. The resulting orange mixture was stirred for 2 h at room temperature, during which time the solids were drawn into solution and an orange-brown solution resulted. The solution was concentrated in vacuo, leaving a dark residue. The crude product was extracted into 4 mL of toluene and filtered through Celite, removing KCl and insoluble impurities. The toluene was removed under vacuum, and by adding Et_2O and hexane a yellow-orange solid was obtained. The volatiles were again removed in vacuo, and the solid was washed with 2 mL of Et_2O at −35 °C, followed by 2 × 2 mL of pentane at room temperature. The product was dried in vacuo. Yield: 77 mg (55%). We were unable to obtain suitable combustion analysis for this compound. The ^{1}H and ^{13}C{^{1}H} NMR spectra are shown in the Supporting Information as evidence for bulk purity. ^{1}H NMR (600 MHz, C_6D_6) δ: 9.41 (d, J = 4.8 Hz, 2H, ArH), 7.21 (d, J = 7.8 Hz, 2H, ArH), 6.98−7.04 (m, 4H, ArH), 6.77−6.84 (m, 4H, ArH), 6.53−6.61 (m, 8H, ArH), 6.44 (t, J = 7.8 Hz, 2H, ArH), 6.20 (d, J = 6.6 Hz, 2H, ArH), 5.48 (d, J = 6.6 Hz, 2H, ArH), 4.80 (s, 1H, PhNC(CH_3)CHC(CH_3)NPh), 1.75 (s, 6H, CH_3). ^{13}C{^{1}H} NMR (151 MHz, $CDCl_3$) δ: 169.7, 158.0, 156.3, 152.3, 150.4, 143.7, 135.9, 132.6, 128.3, 127.3, 127.0, 125.2, 124.3, 123.0, 122.1, 121.0, 119.1, 118.3, 95.0, 25.4. UV−vis (THF): λ/nm (ε/M^{-1} cm^{-1}) 264 (39 000), 357 (12 000), 383 (11 000), 460 (sh) (1800).

Preparation of Ir(ppy)$_2$(acNac^{Me}) (2). A sample of [Ir(ppy)$_2$(μ-Cl)]$_2$ (100 mg, 0.0933 mmol) was suspended in 2 mL of THF. A solution of acNac^{Me}K (40 mg, 0.19 mmol, 2.0 equiv) in 6 mL of THF was added to the stirred mixture. After stirring for 2.5 h at room temperature, a yellow-brown solution was observed, which was concentrated in vacuo. The resulting residue was extracted with 5 mL of toluene and filtered through Celite. The toluene was removed in vacuo, and the residue was washed with 2 mL of Et_2O at −35 °C and 2 × 2 mL of room-temperature pentane, leaving the product as a yellow-orange solid, which was dried in vacuo. Yield: 81 mg (64%). Elemental analysis for this sample showed low carbon content, but the NMR spectra shown in the Supporting Information indicate >95% purity. ^{1}H NMR (600 MHz, C6D$_6$) δ: 9.22 (d, J = 5.4 Hz, 1H, ArH), 8.97 (d, J = 5.4 Hz, 1H, ArH), 7.40 (d, J = 7.2 Hz, 1H, ArH), 7.28 (d, J = 7.2 Hz, 1H, ArH), 7.10 (d, J = 8.4 Hz, 1H, ArH), 6.89−7.00 (m, 3H, ArH), 6.83 (t, J = 7.2 Hz, 1H, ArH), 6.68−6.79 (m, 3H, ArH), 6.51−6.65 (m, 6H, ArH), 6.45 (t, J = 6.9 Hz, 1H ArH), 6.41 (d, J = 7.2 Hz, 1H, ArH), 5.44 (d, J = 7.8 Hz, 1H, ArH), 4.95 (s, 1H, PhNC(CH_3)CHC(O)CH_3), 1.81 (s, 3H, CH_3), 1.58 (s, 3H, CH_3). ^{13}C{^{1}H} NMR (151 MHz, $CDCl_3$) δ: 177.9, 169.3, 169.0, 161.2, 154.3, 152.3, 150.1, 149.6, 148.3, 144.8, 143.8, 136.5, 136.2, 132.9, 132.7, 129.3, 128.5, 127.4, 127.2, 124.2, 123.7, 123.3, 122.6, 122.3, 121.2, 121.0, 120.9, 119.0, 118.6, 118.1, 98.0, 28.0, 24.9. UV−vis (THF): λ/nm (ε/M^{-1}cm^{-1}) 262 (42000), 309 (sh) (17000), 344 (11000), 378 (sh) (7400), 455 (sh) (2400), 492 (1400). Anal. Calcd for $C_{33}H_{28}IrN_3O$: C, 58.74; H, 4.18, N, 6.23. Found: C, 57.02, H, 4.29, N, 5.91.

Preparation of Ir(ppy)$_2$(NacNac^{CF_3}) (3). [Ir(ppy)$_2$(μ-Cl)]$_2$ (100 mg, 0.0933 mmol) and NacNac^{CF_3}Li (68 mg, 0.19 mmol, 2.0 equiv) were combined in 6 mL of toluene and sealed in a Teflon-capped glass tube. The contents were heated to 105 °C with constant stirring for 20 h. During this time most of the solids dissolved, yielding a deep red solution. In the glovebox, the solution was filtered through Celite and concentrated in vacuo. The residue was triturated with Et_2O (2 mL) and the resulting mixture was cooled to −35 °C. After filtration, the dull orange solid was washed with 2 × 2 mL of pentane and dried in vacuo (70 mg yield). After sitting overnight, a second crop of product (13 mg) separated from the combined Et_2O/pentane washings and was collected. Combined Yield: 83 mg (52%). ^{1}H NMR (600 MHz, $CDCl_3$) δ: 9.04 (d, J = 5.4 Hz, 2H, ArH), 7.80 (t, J = 7.8 Hz, 2H, ArH), 7.67 (d, J = 7.2 Hz, 2H, ArH), 7.30 (t, J = 6.3 Hz, 2H, ArH), 7.01 (d, J = 7.8 Hz, 2H, ArH), 6.64 (t, J = 7.2 Hz, 2H, ArH), 6.54 (t, J = 7.2 Hz, 2H, ArH), 6.41−6.51 (m, 6H, ArH), 6.27 (t, J = 7.5 Hz, 2H, ArH), 5.67 (d, J = 7.8 Hz, 2H, ArH), 5.55 (s, 1H, PhNC(CF_3)CHC(CF_3)NPh), 5.31 (d, J = 7.2 Hz, 2H, ArH). ^{13}C{^{1}H} NMR (151 MHz, $CDCl_3$) δ: 169.3, 153.6, 149.4, 148.4, 144.8 (q, $^2J_{CF}$ = 24 Hz), 143.1, 137.1, 132.5, 128.7, 126.7, 126.3, 124.8, 123.5, 123.3, 123.0, 121.6, 121.0 (q, $^1J_{CF}$ = 287 Hz), 120.07, 119.0, 87.2. ^{19}F NMR (565 MHz, $CDCl_3$) δ: −58.9. UV−vis (THF): λ/nm (ε/M^{-1}cm^{-1}) 267 (37000), 334 (sh) (13000), 399 (9000), 417 (sh) (8400), 479 (sh) (3900). Anal. Calcd for $C_{39}H_{27}F_6IrN_4$: C, 54.60; H, 3.17, N, 6.53. Found: C, 54.33, H, 3.27, N, 6.47.

Preparation of Ir(bt)$_2$(NacNac^{Me}) (4). [Ir(bt)$_2$(μ-Cl)]$_2$ (100 mg, 0.0771 mmol) was suspended in 2 mL of THF. A solution of NacNac^{Me}K (45 mg, 0.16 mmol, 2.1 equiv) in 6 mL of THF was added, and the mixture was stirred at room temperature for 2 h, during which time a deep red solution developed. The volatiles were removed in vacuo, leaving a dark red residue. The crude product was extracted with 3 × 2 mL of toluene and filtered through Celite. The toluene was removed under vacuum, and 2 mL of Et_2O were added to the red residue. The product initially dissolved, and upon standing a brick red solid precipitated. The mixture was cooled to −35 °C to encourage further precipitation, and the product was collected by filtration, washed with 2 × 2 mL of pentane, and dried in vacuo. Even after several hours of drying, ^{1}H NMR indicated the presence of 0.33 equiv of Et_2O in the product, which is consistent with the combustion analysis data. Yield: 80 mg (58%). ^{1}H NMR (400 MHz, $CDCl_3$) δ: 8.82 (d, J = 8.4 Hz, 2H, ArH), 7.96 (d, J = 8.4 Hz, 2H, ArH), 7.65 (t, J = 8.1 Hz, 2H, ArH), 7.53 (t, J = 7.8 Hz, 2H, ArH), 7.01 (d, J = 7.8 Hz, 2H, ArH), 6.47−6.58 (m, 8H, ArH), 6.41 (t, J = 7.8 Hz, 2H, ArH), 6.28 (t, J = 7.2 Hz, 2H, ArH), 5.99 (d, J = 7.2 Hz, 2H, ArH), 5.24 (d, J = 7.2 Hz, 2H, ArH), 4.78 (s, 1H, PhNC(CH_3)CHC(CH_3)NPh), 1.62 (s, 6H, CH_3). ^{13}C{^{1}H} NMR (151 MHz, $CDCl_3$) δ: 181.7, 159.1, 157.5, 152.1, 151.7, 141.0, 133.3, 131.7, 129.6, 127.40, 127.37, 126.8, 126.4, 125.0 (2 coincident resonances), 124.9, 122.5, 122.3, 122.1, 119.7, 97.7, 25.3. UV−vis (THF): λ/nm (ε/M^{-1}cm^{-1}) 269 (34000), 291 (sh) (28000), 311 (31000), 322 (32000), 383 (17000), 452 (4600). Anal. Calcd for $C_{43}H_{33}IrN_4S_2$·0.33Et_2O: C, 60.04; H, 4.13, N, 6.32. Found: C, 59.64, H, 4.32, N, 6.14.

Preparation of Ir(bt)$_2$(acNac^{Me}) (5). To a stirred suspension of [Ir(bt)$_2$(μ-Cl)]$_2$ (100 mg, 0.0771 mmol) in 2 mL of THF was added

DOI: 10.1021/acs.inorgchem.5b01401
Inorg. Chem. 2015, 54, 7122−7131

acNac^{Me}K (33 mg, 0.15 mmol, 2.0 equiv) dissolved in 6 mL of THF. The orange mixture was stirred at room temperature for 2 h, with all solids dissolving to yield a red solution. The volatiles were removed in vacuo, leaving a residue which was extracted with 3 × 2 mL of toluene and filtered through Celite. The toluene was removed in vacuo, leaving a sticky red solid. The solid was triturated with Et_2O, and the mixture was chilled to −35 °C before filtering off the orange product. The solid was washed with 2 × 2 mL pentane and dried in vacuo. Even after several hours of drying, the product remained solvated with ca. 0.25 equiv of Et_2O. Yield: 91 mg (73%). ^{1}H NMR (600 MHz, $CDCl_3$) δ: 8.55 (d, J = 7.8 Hz, 1H, ArH), 8.41 (d, J = 8.4 Hz, 1H, ArH), 7.93 (d, J = 8.4 Hz, 1H, ArH), 7.87 (d, J = 7.2 Hz, 1H, ArH), 7.64 (d, J = 7.2 Hz, 1H, ArH), 7.43−7.55 (m, 4H, ArH), 7.04 (d, J = 7.8 Hz, 1H, ArH), 6.83 (t, J = 7.2 Hz, 1H ArH), 6.69 (t, J = 7.2 Hz, 1H, ArH), 6.61 (m, 2H, ArH), 6.55 (t, J = 7.2 Hz, 2H, ArH), 6.41−6.48 (m, 2H, ArH), 6.33 (d, J = 7.8 Hz, 1H, ArH), 6.30 (d, J = 7.2 Hz, 1H, ArH), 5.34 (d, J = 7.8 Hz, 1H, ArH), 4.82 (s, 1H, PhNC(CH_3)CHC(O)CH_3), 1.73 (s, 3H, CH_3), 1.61 (s, 3H, CH_3). ^{13}C{^{1}H} NMR (151 MHz, $CDCl_3$) δ: 181.5, 180.3, 179.2, 163.5, 154.7 153.2, 151.9, 151.3, 149.3, 142.0, 140.9, 134.3, 134.0, 131.6, 131.3, 130.4, 130.0, 127.8, 127.4, 127.3, 126.9, 125.63, 125.56, 125.05, 124.99, 123.9, 123.2, 122.7, 122.5, 122.2, 121.6, 121.3, 120.9, 119.5, 100.3, 27.8, 24.6. UV−vis (THF): λ/nm (ε/M^{-1}cm^{-1}) 277 (35000), 310 (30000), 323 (32000), 339 (sh) (21000), 365 (sh) (11000), 410 (sh) (5900), 493 (sh) (3700). Anal. Calcd for $C_{37}H_{28}IrN_3S_2$·0.25Et_2O: C, 56.66; H, 3.82, N, 5.22. Found: C, 56.40, H, 4.03, N, 5.02.

Preparation of Ir(bt)$_2$(NacNac^{CF_3}) (6). [Ir(bt)$_2$(μ-Cl)]$_2$ (100 mg, 0.0771 mmol) was suspended in a solution of NacNac^{CF_3}Li (56 mg, 0.15 mmol, 2.0 equiv) in 6 mL of toluene, and the resulting mixture was added to a Teflon-capped glass tube. The contents were heated to 110 °C with constant stirring for 14 h. A deep red solution developed, which was allowed to cool to room temperature and filtered through Celite in the glovebox. The toluene was removed in vacuo, leaving an orange/brown solid. The crude product was washed with 2 mL of Et_2O at −35 °C and 2 × 2 mL of pentane at room temperature, leaving a dull orange solid which was dried in vacuo. Yield: 99 mg (66%). ^{1}H NMR (600 MHz, $CDCl_3$) δ: 8.62 (d, J = 9.0 Hz, 2H, ArH), 8.01 (d, J = 7.8 Hz, 2H, ArH), 7.70 (T, J = 7.5 Hz, 2H, ArH), 7.58 (t, J = 7.5 Hz, 2H, ArH), 7.00 (d, J = 7.2 Hz, 2H, ArH), 6.42−6.61 (m, 10H, ArH), 6.32 (t, J = 7.5 Hz, 2H, ArH), 5.86 (d, J = 7.2 Hz, 2H, ArH), 5.76 (s, 1H, PhNC(CF_3)CHC(CF_3)NPh), 5.32 (d, J = 5.4 Hz, 2H, ArH). ^{13}C{^{1}H} NMR (151 MHz, $CDCl_3$) δ: 182.1, 154.2, 151.6, 148.1, 145.8 (q, $^2J_{CF}$ = 25 Hz), 140.5, 133.0, 131.6, 130.1, 127.9, 127.0, 126.4, 125.9, 125.6, 125.3, 123.7, 123.5, 122.8, 121.1, 120.7 (q, $^1J_{CF}$ = 286 Hz), 120.7, 89.6. ^{19}F NMR (565 MHz, $CDCl_3$) δ: −59.1. UV−vis (THF): λ/nm (ε/M^{-1}cm^{-1}) 262 (36000), 269 (35000), 313 (sh) (32000), 322 (37000), 418 (13000), 452 (sh) (8500). Anal. Calcd for $C_{43}H_{27}F_6IrN_4S_2$: C, 53.24; H, 2.81, N, 5.78. Found: C, 53.08, H, 2.96, N, 5.62.

X-ray Crystallography Procedures. Single crystals of **3**−**6** were grown by vapor diffusion of pentane into concentrated THF solutions. Crystals were mounted on a Bruker Apex II three-circle diffractometer using Mo Kα radiation (λ = 0.71073 Å). The data were collected at 123(2) K and processed and refined within the APEXII software. Structures were solved by direct methods in SHELXS and refined by standard difference Fourier techniques in the program SHELXL. Hydrogen atoms were placed in calculated positions using the standard riding model and refined isotropically; all non-hydrogen atoms were refined anisotropically. The structure of **4** contained a disordered solvent molecule at a special position which refined best as *n*-hexane. Distance restraints (SADI) were used for all 1,2 and 1,3 distances within the disordered solvent molecule, and rigid bond restraints SIMU and DELU were employed for the thermal displacement parameters. Crystallographic details are summarized in Tables S1 and S2.

■ ASSOCIATED CONTENT

Supporting Information

Crystallographic summary tables, ^{1}H and ^{13}C{^{1}H} NMR spectra of all new compounds, and individual UV−vis absorption/emission spectra of complexes **1**−**6**. The Supporting Information is available free of charge on the ACS Publications website at DOI: 10.1021/acs.inorgchem.5b01401.

■ AUTHOR INFORMATION

Corresponding Author

*E-mail: tteets@uh.edu.

Notes

The authors declare no competing financial interest.

■ ACKNOWLEDGMENTS

We thank the University of Houston and the Welch Foundation (Grant No. E-1887) for funding this research, and Prof. Loi Do for access to the UV−vis spectrophotometer.

■ REFERENCES

(1) Prier, C. K.; Rankic, D. A.; MacMillan, D. W. C. *Chem. Rev.* **2013**, *113*, 5322−5363.
(2) Zuo, Z.; Ahneman, D. T.; Chu, L.; Terrett, J. A.; Doyle, A. G.; MacMillan, D. W. C. *Science* **2014**, *345*, 437−440.
(3) Yoon, T. P.; Ischay, M. A.; Du, J. *Nat. Chem.* **2010**, *2*, 527−532.
(4) Zhao, Q.; Huang, C.; Li, F. *Chem. Soc. Rev.* **2011**, *40*, 2508−2524.
(5) Baggaley, E.; Weinstein, J. A.; Williams, J. A. G. *Coord. Chem. Rev.* **2012**, *256*, 1762−1785.
(6) Yang, Y.; Zhao, Q.; Feng, W.; Li, F. *Chem. Rev.* **2013**, *113*, 192−270.
(7) Maity, A.; Choi, J.-S.; Teets, T. S.; Deligonul, N.; Berdis, A. J.; Gray, T. G. *Chem. - Eur. J.* **2013**, *19*, 15924−15932.
(8) *Highly efficient OLEDs with phosphorescent materials*; Yersin, H., Ed.; Wiley-VCH: Weinheim, 2008.
(9) Lamansky, S.; Djurovich, P.; Murphy, D.; Abdel-Razzaq, F.; Lee, H.-E.; Adachi, C.; Burrows, P. E.; Forrest, S. R.; Thompson, M. E. *J. Am. Chem. Soc.* **2001**, *123*, 4304−4312.
(10) Lowry, M. S.; Bernhard, S. *Chem. - Eur. J.* **2006**, *12*, 7970−7977.
(11) Dedeian, K.; Djurovich, P. I.; Garces, F. O.; Carlson, G.; Watts, R. J. *Inorg. Chem.* **1991**, *30*, 1685−1687.
(12) Tamayo, A. B.; Alleyne, B. D.; Djurovich, P. I.; Lamansky, S.; Tsyba, I.; Ho, N. N.; Bau, R.; Thompson, M. E. *J. Am. Chem. Soc.* **2003**, *125*, 7377−7387.
(13) Maity, A.; Anderson, B. L.; Deligonul, N.; Gray, T. G. *Chem. Sci.* **2013**, *4*, 1175−1181.
(14) Lamansky, S.; Djurovich, P.; Murphy, D.; Abdel-Razzaq, F.; Kwong, R.; Tsyba, I.; Bortz, M.; Mui, B.; Bau, R.; Thompson, M. E. *Inorg. Chem.* **2001**, *40*, 1704−1711.
(15) Li, J.; Djurovich, P. I.; Alleyne, B. D.; Yousufuddin, M.; Ho, N. N.; Thomas, J. C.; Peters, J. C.; Bau, R.; Thompson, M. E. *Inorg. Chem.* **2005**, *44*, 1713−1727.
(16) Lowry, M. S.; Hudson, W. R.; Pascal, R. A.; Bernhard, S. *J. Am. Chem. Soc.* **2004**, *126*, 14129−14135.
(17) Nazeeruddin, M. K.; Humphry-Baker, R.; Berner, D.; Rivier, S.; Zuppiroli, L.; Graetzel, M. *J. Am. Chem. Soc.* **2003**, *125*, 8790−8797.
(18) Shavaleev, N. M.; Monti, F.; Scopelliti, R.; Baschieri, A.; Sambri, L.; Armaroli, N.; Grätzel, M.; Nazeeruddin, M. K. *Organometallics* **2013**, *32*, 460−467.
(19) Bradley, A. Z.; Merlo, J. A. U.S. Pat. Appl. 20080058517 A1, 2008.
(20) Bourget-Merle, L.; Lappert, M. F.; Severn, J. R. *Chem. Rev.* **2002**, *102*, 3031−3066.
(21) Chamberlain, B. M.; Cheng, M.; Moore, D. R.; Ovitt, T. M.; Lobkovsky, E. B.; Coates, G. W. *J. Am. Chem. Soc.* **2001**, *123*, 3229−3238.

DOI: 10.1021/acs.inorgchem.5b01401
Inorg. Chem. 2015, 54, 7122−7131

(22) Hayes, P. G.; Piers, W. E.; McDonald, R. *J. Am. Chem. Soc.* **2002**, *124*, 2132−2133.
(23) Li, X.-F.; Dai, K.; Ye, W.-P.; Pan, L.; Li, Y.-S. *Organometallics* **2004**, *23*, 1223−1230.
(24) Cui, C.; Roesky, H. W.; Schmidt, H.-G.; Noltemeyer, M.; Hao, H.; Cimpoesu, F. *Angew. Chem., Int. Ed.* **2000**, *39*, 4274−4276.
(25) Driess, M.; Yao, S.; Brym, M.; van Wüllen, C.; Lentz, D. *J. Am. Chem. Soc.* **2006**, *128*, 9628−9629.
(26) Holland, P. L.; Tolman, W. B. *J. Am. Chem. Soc.* **1999**, *121*, 7270−7271.
(27) MacLeod, K. C.; Vinyard, D. J.; Holland, P. L. *J. Am. Chem. Soc.* **2014**, *136*, 10226−10229.
(28) Basuli, F.; Bailey, B. C.; Tomaszewski, J.; Huffman, J. C.; Mindiola, D. J. *J. Am. Chem. Soc.* **2003**, *125*, 6052−6053.
(29) Thompson, R.; Chen, C.-H.; Pink, M.; Wu, G.; Mindiola, D. J. *J. Am. Chem. Soc.* **2014**, *136*, 8197−8200.
(30) Kogut, E.; Wiencko, H. L.; Zhang, L.; Cordeau, D. E.; Warren, T. H. *J. Am. Chem. Soc.* **2005**, *127*, 11248−11249.
(31) Jang, E. S.; McMullin, C. L.; Käß, M.; Meyer, K.; Cundari, T. R.; Warren, T. H. *J. Am. Chem. Soc.* **2014**, *136*, 10930−10940.
(32) Sudhakar, M.; Djurovich, P. I.; Hogen-Esch, T. E.; Thompson, M. E. *J. Am. Chem. Soc.* **2003**, *125*, 7796−7797.
(33) Juris, A.; Balzani, V.; Barigelletti, F.; Campagna, S.; Belser, P.; von Zelewsky, A. *Coord. Chem. Rev.* **1988**, *84*, 85−277.
(34) Gussenhoven, E. M.; Olmstead, M. M.; Fettinger, J. C.; Balch, A. L. *Inorg. Chem.* **2008**, *47*, 4570−4578.
(35) Lucas, S. J.; Lord, R. M.; Wilson, R. L.; Phillips, R. M.; Sridharan, V.; McGowan, P. C. *Dalton Trans.* **2012**, *41*, 13800−13802.
(36) Budzelaar, P. H. M.; de Gelder, R.; Gal, A. W. *Organometallics* **1998**, *17*, 4121−4123.
(37) Bernskoetter, W. H.; Lobkovsky, E.; Chirik, P. J. *Chem. Commun.* **2004**, 764−765.
(38) Ohsawa, Y.; Sprouse, S.; King, K. A.; DeArmond, M. K.; Hanck, K. W.; Watts, R. J. *J. Phys. Chem.* **1987**, *91*, 1047−1054.
(39) Dixon, I. M.; Collin, J.-P.; Sauvage, J.-P.; Flamigni, L.; Encinas, S.; Barigelletti, F. *Chem. Soc. Rev.* **2000**, *29* (6), 385−391.
(40) Zuo, Z.; MacMillan, D. W. C. *J. Am. Chem. Soc.* **2014**, *136*, 5257−5260.
(41) Nguyen, J. D.; Matsuura, B. S.; Stephenson, C. R. J. *J. Am. Chem. Soc.* **2014**, *136*, 1218−1221.
(42) Nazeeruddin, M. K.; Wegh, R. T.; Zhou, Z.; Klein, C.; Wang, Q.; De Angelis, F.; Fantacci, S.; Grätzel, M. *Inorg. Chem.* **2006**, *45*, 9245−9250.
(43) De Angelis, F.; Fantacci, S.; Evans, N.; Klein, C.; Zakeeruddin, S. M.; Moser, J.-E.; Kalyanasundaram, K.; Bolink, H. J.; Grätzel, M.; Nazeeruddin, M. K. *Inorg. Chem.* **2007**, *46*, 5989−6001.
(44) Glazer, E. C.; Magde, D.; Tor, Y. *J. Am. Chem. Soc.* **2005**, *127*, 4190−4192.
(45) Glazer, E. C.; Magde, D.; Tor, Y. *J. Am. Chem. Soc.* **2007**, *129*, 8544−8551.
(46) Sun, Y.; Liu, Y.; Turro, C. *J. Am. Chem. Soc.* **2010**, *132*, 5594−5595.
(47) Denisov, S. A.; Cudré, Y.; Verwilst, P.; Jonusauskas, G.; Marín-Suárez, M.; Fernández-Sánchez, J. F.; Baranoff, E.; McClenaghan, N. D. *Inorg. Chem.* **2014**, *53*, 2677−2682.
(48) We cannot rigorously exclude the possibility that the high-energy emission bands, whose excitation profiles bear less of a resemblance to the absorption spectra, are attributed to a highly emissive impurity. The energy and shape of these bands do exclude $Ir(C^N)_3$ and $[Ir(C^N)_2(\mu\text{-}Cl)]_2$ as the culprits.
(49) Pangborn, A. B.; Giardello, M. A.; Grubbs, R. H.; Rosen, R. K.; Timmers, F. J. *Organometallics* **1996**, *15*, 1518−1520.
(50) Tang, L.-M.; Duan, Y.-Q.; Li, X.-F.; Li, Y.-S. *J. Organomet. Chem.* **2006**, *691*, 2023−2030.
(51) Carey, D. T.; Cope-Eatough, E. K.; Vilaplana-Mafé, E.; Mair, F. S.; Pritchard, R. G.; Warren, J. E.; Woods, R. J. *Dalton Trans.* **2003**, 1083−1093.
(52) Bailey, P. J.; Coxall, R. A.; Dick, C. M.; Fabre, S.; Henderson, L. C.; Herber, C.; Liddle, S. T.; Loroño-González, D.; Parkin, A.; Parsons, S. *Chem. - Eur. J.* **2003**, *9*, 4820−4828.
(53) Martin, D. F.; Janusonis, G. A.; Martin, B. B. *J. Am. Chem. Soc.* **1961**, *83*, 73−75.
(54) Adhikari, D.; Tran, B. L.; Zuno-Cruz, F. J.; Cabrera, G. S.; Mindiola, D. J. *Inorg. Synth.* **2010**, *35*, 8−13.
(55) Tinker, L. L.; McDaniel, N. D.; Cline, E. D.; Bernhard, S. *Inorg. Synth.* **2010**, *35*, 168−173.
(56) A Guide to Recording Fluorescence Quantum Yields. http://www.horiba.com/fileadmin/uploads/Scientific/Documents/Fluorescence/quantumyieldstrad.pdf (accessed May 2015).
(57) Seybold, P. G.; Gouterman, M. *J. Mol. Spectrosc.* **1969**, *31*, 1−13.

DOI: 10.1021/acs.inorgchem.5b01401
Inorg. Chem. 2015, 54, 7122−7131